Malaysian Journal of Chemistry, 2024, Vol. 26(5), 562-571
(Special Issue: *4th IKMPB Online Symposium 2024 - Development of Chemistry to Accomplish a Sustainable World*)

Effect of Sulphuric Acid Concentration on Nanocellulose Extraction from Rice Husk

Anis Sofiya Zulkifli[1], Nurul Asyikin Abd Halim[1], Shariff Ibrahim[1,2], Noraini Hamzah[1,2] and Sabiha Hanim Saleh[1,2]*

[1]Department of Chemistry and Environment, Faculty of Applied Sciences, Universiti Teknologi MARA, 40450 Shah Alam, Selangor, Malaysia

[2]Industrial Waste Conversion Technology Research Group, Faculty of Applied Sciences, Universiti Teknologi MARA, 40450 Shah Alam, Selangor, Malaysia

*Corresponding author: sabihahanim@uitm.edu.my

In this study, nanocellulose (NC) was produced chemically from rice husk (RH) by alkaline extraction, bleaching, and acid hydrolysis. The effect of different sulphuric acid (H_2SO_4) concentrations (8%, 10%, 12%, 14%, and 16%) on the yield of NC was examined. The characteristics of NC were studied using Fourier transform infrared (FTIR) spectroscopy, field emission scanning electron microscopy (FESEM), X-ray diffraction (XRD), and thermogravimetric analysis (TGA). The highest NC yield was obtained at 12% H_2SO_4. The FTIR spectra of NC showed prominent peaks corresponding to cellulose. Based on FESEM analysis, NC constituted a rod-like structure that was completely cleaved in a range of 12%–16% H_2SO_4. The TEM analysis showed the NC fibre was found to be in the range of 8–50 nm. The XRD analysis demonstrated that the crystallinity index and crystallite size of NC increased when the H_2SO_4 concentration increased up to 12%. The primary XRD peaks at 2θ = 18°, 22°, and 34° were not affected during acid hydrolysis. The thermal degradation of all NC samples was higher than the raw RH, showing that the NC was stable at high temperatures of more than 300 °C; however, as H_2SO_4 concentration increased, the thermal stability decreased. Different H_2SO_4 concentrations give significant changes to the physicochemical properties of NC from RH.

Keywords: Nanocellulose; acid hydrolysis; crystallinity; rice husk

Received: January 2024; Accepted: July 2024

Rice husk (RH) is one of the agricultural wastes obtained from rice milling industries in Malaysia, which can be used as a source for cellulose extraction. The annual worldwide rice paddy manufacturing is 741 million tons, producing approximately 148 million tons of RH. Rice husk includes approximately 38% cellulose, 25% hemicellulose, 20% lignin, and 17% ash, of which 94% is silica. Rice husk is regularly left as waste or burned for the use of crude supply of energy, fertiliser, grain, and as an insulator in the brick industry. Rice milling industries sometimes dispose of RHs by open burning. This practice raises environmental concerns and poses significant risks, causing damage to the land and surrounding environment [1]. Researchers are increasingly interested in applying technology to reprocess agricultural waste for a cleaner environment. Conducting research using RH as a raw material is worthwhile as it offers better dimensional stability in response to moisture and exposure [2].

Cellulose is the most abundant biopolymer on earth, and it is a renewable natural polymer that is made up of polysaccharides containing a linear chain of β-1,4 linked D-glucose of repeating units called anhydroglucose units. Cellulose is packed inside microfibrils' (diameter of 0.1–1.0 μm) plant cell wall that is held together by intra- and intermolecular hydrogen bonds, as well as intermolecular van der Waals forces. In addition, nanocellulose (NC) can be further extracted from cellulose. The size range of NC (10–70 nm) is much smaller than cellulose [3]. Nanocellulose can exist in the form of cellulose nanocrystals (CNCs), which have a short and rigid crystalline rod-like structure, and cellulose nanofibres, which have a more entangled, long, and flexible structure [4]. Nanocellulose is an outstanding material that has a high aspect ratio, greater mechanical properties, and is biodegradable. In addition, RH has the potential to be a good feedstock for NC [1]. The production of NC with a nano-scale size is what makes NC a distinguished green material. Thus, NC is most likely to be selected in this study over cellulose due to the added value of NC and its properties. Such an application would contribute to waste management of the significant rice industry waste.

Efficient treatment methods are critical in extracting NC from RH due to the presence of a great number of impurities like dust [5]. Due to the high energy consumption of mechanical techniques, acid hydrolysis was used in this study to obtain NC as it is

†Paper presented at the 4th IKMPB Online Symposium 2024 – Development of Chemistry to Accomplish a Sustainable World

an easy operation technique [4]. Furthermore, by dissolving the disordered part (i.e., amorphous cellulose) in cellulose and the ordered part (i.e., nanocrystal cellulose) in the remaining part, acid hydrolysis using sulphuric acid (H_2SO_4) can successfully isolate nanocrystalline cellulose, producing a stable colloid system due to the hydroxyl group esterification by sulphate ions [6]. The primary influencing factor in this study is applying different H_2SO_4 concentrations. It results in different morphology and yield of the NC obtained. Typically, NC is produced at high H_2SO_4 concentrations (50%–64%), low temperature (45 °C), and reaction time of 60 min. However, in this study, lower H_2SO_4 concentrations were employed at a temperature of 45 °C, and the hydrolysis time was set to 130 min. The bleaching process used hydrogen peroxide (H_2O_2), which is more environmentally friendly compared to sodium chlorite. The effect of different H_2SO_4 concentrations on the yield and physicochemical properties of NC from RH was studied. Subsequently, the characterisation of NC particles was conducted using field emission scanning electron microscopy (FESEM), transmission electron microscopy (TEM), X-ray diffraction (XRD), Fourier transform infrared (FTIR) spectroscopy, and thermogravimetric analysis (TGA).

EXPERIMENTAL

Chemicals and Materials

Rice husk was obtained from a local paddy field in Perak, Malaysia. The RH was first washed six times with distilled water and oven-dried for 12 h at 60 °C, and then milled and sieved using a mill blade to obtain particle sizes of 100–240 µm. The sample contained 48.93% cellulose, 21.09% hemicellulose, 19.97% Klason lignin, and 9.11% extractives. The dried samples were kept in a tight container prior to use. The chemicals used in this study were of analytical grade unless otherwise stated.

Alkaline Treatment

Alkaline treatment using sodium hydroxide (NaOH) was performed to isolate cellulose from RH by removing lignin and hemicellulose, as reported by Kaur [7] with some modifications. The milled and sieved RH (approximately 30 g) was treated with 4% (w/v) NaOH in a water bath at 80 °C for 1 h with a RH-to-NaOH solution ratio of 1:20 (w/v) and subsequently stirred. The mixture was then vacuum-filtered, and the filtrate was washed several times using distilled water until a neutral pH was achieved. Following that, the alkali-treated RH was oven-dried for 2 h at 50 °C.

Bleaching Treatment

The chlorine-free method was employed to bleach the alkali-treated RH, as reported by Benini [8]. The alkali-treated RH was bleached three times. The ratio of RH to solution was 1:20 (g/mL), where 24% (v/v) of H_2O_2 and 4% (w/w) of NaOH (1:1 solution of H_2O_2 and NaOH) were used to bleach the RH at 50 °C under constant stirring for 2 h. The residue was filtered and washed several times with distilled water until a neutral pH was achieved. The final product (cellulose) was oven-dried at 60 °C for 48 h and stored for acid hydrolysis treatment.

Acid Hydrolysis

Rice husk NC was extracted by acid hydrolysis via a modified method [9-10]. First, 2 g of the cellulose obtained from the bleaching treatment was hydrolysed with four different H_2SO_4 concentrations (8% (v/v), 10% (v/v), 12% (v/v), and 14% (v/v)) under magnetic stirring (500 rpm) for 130 min in a water bath at 45 °C. Afterwards, all mixtures were diluted with 500 mL of distilled water to stop the acid hydrolysis process. The suspensions were centrifuged at 4,000 rpm for 25 min at 10 °C to remove the remaining acids. The resulting samples were dialysed in a dialysis membrane tube using distilled water for more than 10 days to neutralise the suspensions by which the water was changed daily. All samples were collected only after the pH of the samples was close to neutral. The samples were then sonicated for 10 min at 25 °C.

The yield of RH nanocellulose of the samples was calculated using Equation 1:

$$\text{Yield of nanocellulose} = \frac{W_f}{W_i} \times 100\% \quad \text{Equation 1}$$

Where W_f is the final weight of NC after freeze-drying and W_i is the initial weight of cellulose subjected to acid hydrolysis.

Characterisation of RH Nanocellulose

Fourier Transform Infrared Spectroscopy

Fourier transform infrared spectra were obtained using a Perkin-Elmer FTIR spectrometer (Perkin Elmer, USA). The FTIR technique was used to determine the presence of the functional groups of raw RH and NC from different concentrations of acid hydrolysis. The samples were finely ground and mixed with potassium bromide (KBr) to form a KBr pellet after compression. The wavenumber for the five samples was set in the range of 400–4000 cm^{-1} [7].

Field Emission Scanning Electron Microscopy

The treated samples were analysed using a field emission scanning electron microscope (Zeiss, Merlin) at a 30 kV acceleration voltage and 1.6 nm. An iridium coating was applied to the sample using an ion sputter coater prior to analysis.

Transmission Electron Microscopy

The TEM analysis was performed using an FEI Talos L120C transmission electron microscope fitted with a 120 kV emission gun. The sample was placed in ethanol and sonicated using a sonicator probe to break down the bonds between particles for 10 min. Approximately 100 µL of the sample solution was dropped onto the carbon mesh formvar copper grid in three drops and allowed to dry at room temperature. The images were controlled using Velox software (Thermo Fisher) and viewed using the bright-field mode at 120 kV and magnification at 100 nm.

X-Ray Diffraction

The changes in the crystallinity of RH nanocellulose at different H_2SO_4 concentrations were determined by an XRD instrument (Malvern Panalytical, UK) with Cu-Kα radiation generated at 45 kV and 40 mA. The scanning range applied was 2θ = 10–90° at a scanning speed of 0.3°/s. The RH nanocellulose suspension from different H_2SO_4 concentrations was freeze-dried at -30 °C to attain dry powder NC particles [9]. The Segal equation in Equation 2 was used to calculate the crystallinity index (CI) of every sample that consists of different peaks in one diffractogram.

$$CI\ (\%) = 100\% \times \frac{I_{101} - I_{am}}{I_{101}} \qquad \text{Equation 2}$$

Where I_{101} is the maximum intensity of the principal peak (101) having a reference value of 2θ = 22° and I_{am} is the intensity of the amorphous peak between crystalline planes (002) and (101) (2θ = 18°). The average crystallite size of NC (L) was determined using the Scherrer's equation, as shown by Equation 3 [10].

$$L = {}^{K\lambda}/_{\beta Cos\theta} \qquad \text{Equation 3}$$

Where K is a correction factor with a value of 0.91, λ is the wavelength of the X-ray source (0.154 Å), θ is the diffraction angle, and β is the full-width at half-maximum of the peak corresponding to the crystalline plane (002) (2θ = 22°).

Thermogravimetric Analysis

The thermal stability of RH nanocellulose was measured using TGA (SETARAM, France). This instrument was used to conduct the analysis that utilises the nitrogen atmosphere. In this analysis, 10 mg of each RH nanocellulose sample was used for the analysis at a constant heating rate of 20 °C/min between 20 and 600 °C with a gas flow rate of 60 mL/min. The TGA thermal curve was displayed as weight percent (%) versus temperature.

RESULTS AND DISCUSSION

After undergoing several chemical treatments including alkaline treatment, bleaching, and acid hydrolysis, the brownish colour of the RH changed to yellowish white. Figure 1 illustrates the stages of converting RH into NC. The yield of cellulose after alkali treatment and bleaching was 64.11%. Table 1 shows the yield of NC from RH under different H_2SO_4 concentrations. The yield of NC increased as the concentration of H_2SO_4 increased. The highest yield of NC was 84.18% when the H_2SO_4 concentration increased up to 12%. However, with a further increase of H_2SO_4 concentration from 12% to 14%, the yield gradually decreased. This could be due to cellulose degradation into other by-products. According to several previous studies, hydrolysis proceeds more efficiently when acid content, time, and temperature increase [11]. However, if the acid concentration increases in a longer and heated condition, it will cause further degradation of cellulose into sugar, such as glucose, resulting in a lower yield [12].

Nanocellulose conversion typically requires a higher acid concentration to achieve a higher yield; however, as RH has a lower lignin content compared to other woody plants, a lower acid concentration is appropriate for acid hydrolysis [13]. Rice husk with low lignin content is easier to process because there are fewer barriers to overcome, allowing for more efficient extraction of cellulose into NC. However, a longer reaction time is needed for acid hydrolysis to maximise the cellulose conversion into NC [12].

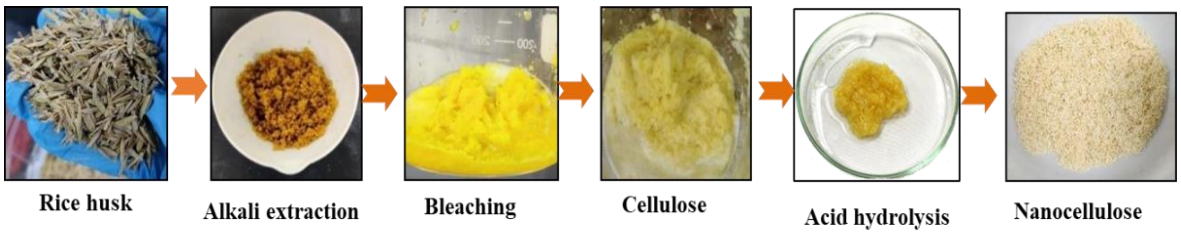

Figure 1. Visual states of RH during different stages of extraction.

Table 1. Yield of RH nanocellulose at different H_2SO_4 concentrations.

Samples	H_2SO_4 concentration (%v/v)	Nanocellulose Yield (%)
8NC	8%	81.07 ± 1.51
10NC	10%	82.61 ± 1.94
12NC	12%	84.18 ± 0.45
14NC	14%	81.56 ± 1.15
16NC	16%	80.15 ± 1.24

Characterisation

FTIR Analysis

An IR absorption spectrum identifies functional groups based on absorbed bands, implying the chemical structure of a molecule. The goal of the FTIR study was to validate that lignin and hemicelluloses were eliminated throughout the chemical modification procedure. Initially, the bleaching treatment isolated cellulose in NC production. The FTIR spectra of raw RH and four different NCs are shown in Figure 2. The peak in the FTIR spectra of raw RH at 3400 cm^{-1} revealed the O–H stretching of cellulose and hemicellulose hydroxyl groups, which had been weakened by acid hydrolysis, suggesting the elimination of hemicellulose. The peak intensity of cellulose and NC at 3400 cm^{-1} was less intense. The strength of these absorption peaks decreased which might be attributed to the chemical reaction of exposed -OH groups with the alkali, bleaching, and acid hydrolysis treatments. The peak at 2925–2898 cm^{-1} corresponds to the C–H stretching of methyl cellulose and methylene groups, which decreased after alkaline and bleaching treatments.

Wax and natural lipids that are represented in the RH wall membrane are associated with the carbonyl (C=O) vibration from the carboxylic groups in the acetyl and uronic ester groups of hemicellulose or to the bonds between the ester groups of lignin or hemicellulose at 1635 cm^{-1}. The peak intensity in this absorption vibration range was shown to decrease after treatments, indicating that the carboxyl groups present in lignin or hemicellulose were removed [14]. Moreover, the typical peak at 1515 cm^{-1} in raw RH represented C=C stretching, which was attributed to aromatic lignin or xylan that diminished in intensity when hemicellulose and lignin were removed by acid hydrolysis [10]. Three distinct mechanisms may occur during NC synthesis [15]. First, SO_4^{2-} targets C-6 of the cellulose pyranose ring because there is less steric disruption at C-6 than at other carbon ring sites. This is supported by an S=O peak at 1205 cm^{-1} as a result of increasing the H_2SO_4 concentration from 8% to 16%. The H^+ ions attack the glycosidic linkages, causing the cellulose chains to break down, resulting in NC production.

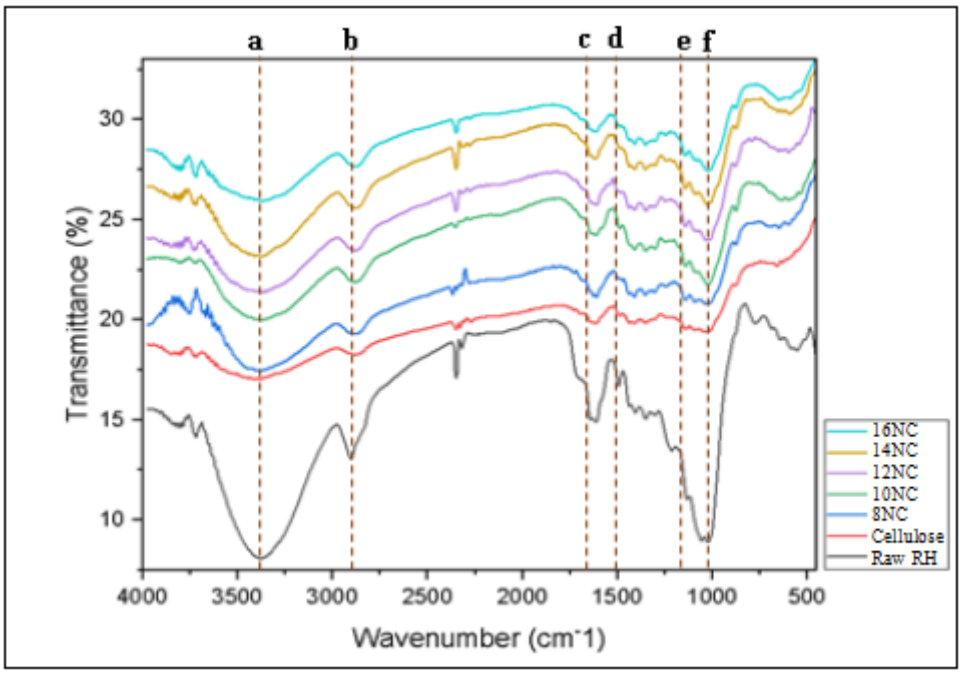

Figure 2. The FTIR spectra of raw RH, cellulose, and four different NCs.

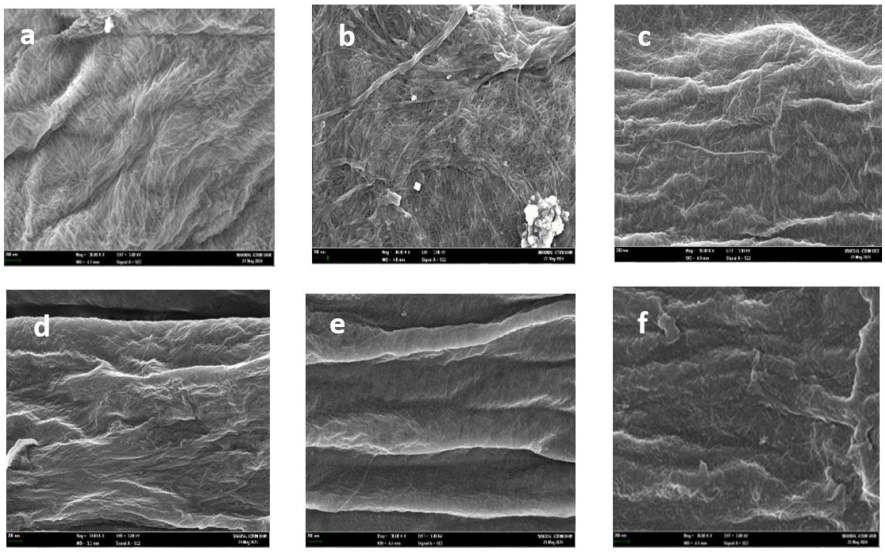

Figure 3. FESEM morphology of a) cellulose, b) 8NC, c) 10NC, d) 12NC, e) 14NC, and f) 16NC.

Finally, hydrolysis might have occurred at the C–O–C pyranose ring skeleton and ruptured the cellulosic ring. The reduced intensity at the 1045 cm^{-1} band revealed its occurrence at the C–O–C pyranose ring. There were no significant differences in the spectra corresponding to raw RH, cellulose, and all NCs. The results revealed that the molecular structure of cellulose and all NCs did not change much after bleaching and acid hydrolysis. The chemical treatments preserved the primary structure of the cellulose backbone, and the finding is consistent with the finding reported by other researchers [16-17].

Surface Morphology

The FESEM study revealed the surface morphological features of NC. Figure 3 depicts the FESEM images of cellulose and NCs at various H_2SO_4 concentrations. Some of the changes could be observed in the characteristics and surface area from cellulose to NC as the concentration of H_2SO_4 increased (8%–16%). The surface of cellulose (Figure 3(a)) after alkaline treatment and bleaching exhibited a smaller layer of fibrils and a well-arranged structure. The results of NC (Figure 3(b–f)), which were obtained after acid hydrolysis of cellulose, elucidated significant differences between cellulose.

The morphology of all NCs showed irregular surface of fibres. All these hydrolysis conditions combined to form a network-like structure. This network-forming capacity of NC is crucial as it is associated with a strong reinforcement when utilised in polymeric composites [7]. Additionally, 8NC and 10NC displayed partial cleaves of the fibre, indicating that these conditions did not fully disrupt the cellulose fibre structures. Meanwhile, for 12NC, 14NC, and 16NC, the fibre had been cleaved and could portray the removal of the amorphous region, resulting in the formation of separated fibrils. Based on the observation, H^+ ions attack the glycosidic connections of cellulose chains, causing the scissoring effect of polymeric chains and the production of single fibre structures of the NC [15]. The higher concentration of acid used in extracting NC produced a less-arranged fibril structure. The large surface area, fibrous structure, and high porosity of NCs from the removal of amorphous regions led to significant adsorption [18].

TEM Analysis

Figure 4 presents the TEM images of the NC obtained from the hydrolysis of cellulose with different H_2SO_4 concentrations. The TEM micrograph analysis indicated that the aqueous suspension of NC fibres comprised rod-like nanoparticles. Some nanoparticles agglomerated in the form of bundles, while others were found to be well-separated. The NC fibre was found to be in the range of 8–50 nm, thus proving that they are in nanoscale. Some locations in the TEM images revealed stacking or blocking due to the high specific surface area of NC and hydrogen bonding between the hydroxyl groups on the molecular chains [19, 20]. The morphology of the NC obtained in this study is similar to the NC produced via acid hydrolysis in a previous study [21].

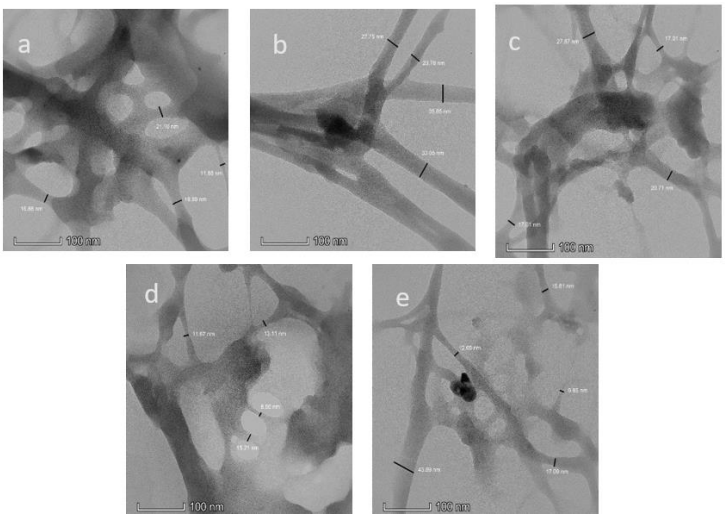

Figure 4. TEM morphology of a) 8NC, b) 10NC, c) 12NC, d) 14NC, and e) 16NC.

XRD Analysis

The X-ray diffractograms of raw RH, cellulose, and NCs are shown in Figure 5. The samples depicted peaks at 2θ = 16°, 22°, and 34°, which could be assigned to crystallographic planes (002), (101), and (200), respectively. These three peaks with a major peak at 2θ = 22° represented cellulose I allomorphism. A similar pattern was observed for the cellulose I structure in another study [10]. The results obtained were broad-humped and noisy diffractograms, which showed that the RH sample was an amorphous material. The removal of non-cellulosic components during the extraction process might cause the XRD peaks to shift. No shifting was observed in this study, indicating that lignin and hemicellulose did not affect the natural crystalline structure of cellulose in the RH sample. Furthermore, no polymorphic alteration of cellulose was seen during the extraction procedures, suggesting that cellulose I remained stable throughout the process. This proved that the chemical treatment did not influence the cellulose structure.

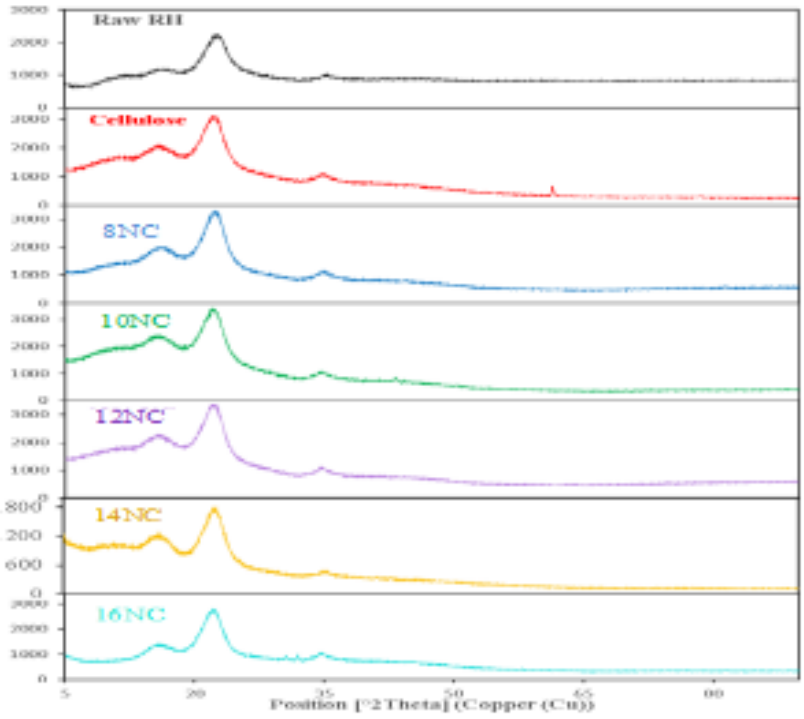

Figure 5. X-ray diffractograms of raw RH, cellulose, and NCs at different H_2SO_4 concentrations.

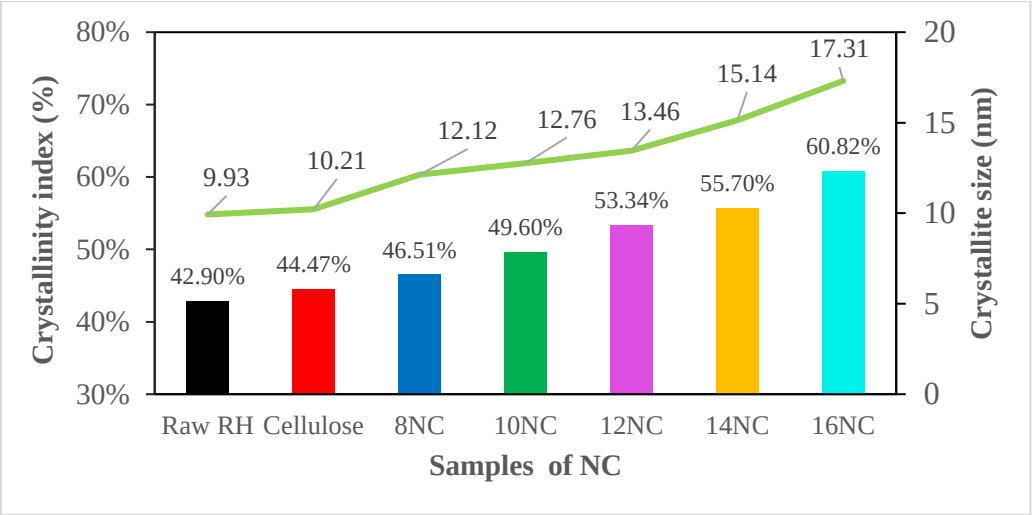

Figure 6. Crystallinity index and crystallite size of raw RH, cellulose, and NCs at different H_2SO_4 concentrations.

The CI and crystallite size of raw RH, cellulose, and NCs are shown in Figure 6. The CI and crystallite size of NC samples were analysed using XRD analysis. The inter- and intra-hydrogen bonding, as well as the van der Waals interaction between the polymeric chains, contributed to the formation of the NC crystalline form [15]. The raw RH had the lowest CI (42.90%) compared to cellulose and NC samples (44.47%–60.82%). The peak intensity decreased when H_2SO_4 concentration increased from 12% to 16%. Similar observations of CI were also made by other researchers [10] during solvent extraction, alkali treatment, bleaching, and acid hydrolysis of RH for medium-sized grain at 44.23% (raw RH), 59.79% (cellulose), and 62.32% (NC). Islam [22] reported that the CI values for raw RH, delignified, bleached, and NC of RH were 33.4%, 43.3%, 52.6%, and 61.6%, respectively.

All findings exhibited similar results, where acid hydrolysed would give the highest CI. This distinction is attributed to the presence of embedded amorphous lignin and hemicellulose in contrast to crystalline cellulose. It was expected that the treated RH (cellulose and NCs) would have higher crystallinity than raw RH as more hydrogen bonding is present in the samples. This made the treated RH to be more densely packed with fibril linkages. Alkaline treatment, bleaching, and acid hydrolysis resulted in partial removal of lignin and hemicellulose during chemical treatment, and this finding is in agreement with a study by [23]. Instead of dissolving crystalline domains, dilute acid treatment dissolved the amorphous region of cellulose. Hydronium ions entered the amorphous region of cellulose, allowing hydrolytic fragmentation of glycosidic linkages and the production of individual crystallites. The development and alignment of monocrystals is consistent with cellulose crystallinity, where a greater CI resulted in a larger crystallite size. The strength and rigidity of cellulose increased when the crystallite size and CI increased. Moreover, 16NC showed the highest crystallite size of 17.31 nm compared to the other nanocellulose. A study by [15] reported similar results, where the CI increased as the concentration of acid increased. The stiffness and rigidity of cellulose increased when the crystallite size and CI increased. The crystallite size for the NC of medium grain from RH was determined as 14.54 nm [10].

Thermal Analysis

Thermogravimetric analysis provides information on the thermal stability of raw RH, cellulose, and four different NCs. The TGA thermogram is shown in Figure 7. All samples exhibited initial weight loss (first stage) between 60 and 140 °C regardless of their treatment conditions. This is due to the vaporisation of chemisorbed and intermolecular hydrogen-bonded water [10]. In contrast to raw RH (280.2 °C), the degradation of the treated RH occurred at higher temperatures of 310.5 °C for cellulose and 325–365 °C for NC samples (Table 2). This suggests that the treated RH had improved thermal stability. From the thermogram, it could be depicted that 16NC had the lowest thermal degradation at 325 °C among other NC samples. The thermal stability of 8NC to 16NC decreased as H_2SO_4 concentrations increased from 8% to 16%. Collazo-Bigliardi [24] reported that cellulose decomposition primarily occurred between 275 and 350 °C, and they found that the thermal degradation of untreated RH occurred at 247.6 °C (first stage) and 301.8 °C (second stage), while the thermal degradation of alkali-treated RH, bleached RH, and CNC occurred at 263.0 °C, 292.4 °C, and 261.8 °C, respectively.

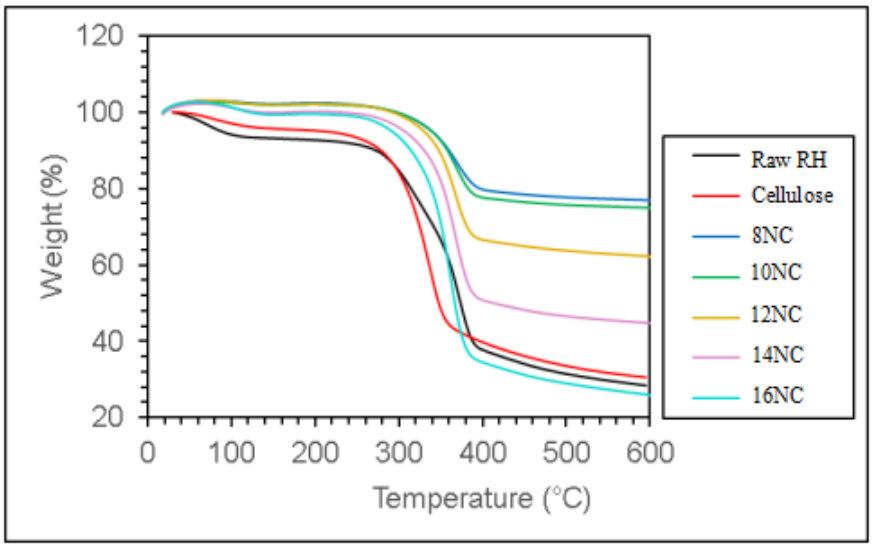

Figure 7. TGA curves of raw RH, cellulose, and NCs at different H_2SO_4 concentrations.

Table 2. Onset temperatures for the thermal degradation of raw RH, cellulose, and NCs at different H_2SO_4 concentrations.

Samples	260 – 400 °C
	Tonset (°C)
Raw RH	280.2
Cellulose	310.5
8NC	365.0
10NC	360.0
12NC	345.0
14NC	342.0
16NC	325.0

A report by [15] indicated a similar decomposition temperature with this study, where the sample produced at the highest H_2SO_4 concentration (78%) exhibited the lowest thermal stability (180 °C) as the C-6 in glucose units reacted with SO_3^-. Sulphate groups (SO_3^-) were found on the outer surface of NC cellulose chains after hydrolysis with H_2SO_4. The inclusion of SO_3^- significantly reduced thermal stability via dehydration. As a result, 14NC and 16NC with higher SO_4^{3-} ratios decreased the thermal degradation temperature.

CONCLUSIONS

The best H_2SO_4 concentration for hydrolysing cellulose to NC is 12% H_2SO_4, resulting in an NC yield of 84.18%. All samples were examined for their functional groups, morphology, crystallinity, and thermal stability. All samples exhibited similar molecular structure, except the presence of S=O in NC samples and the diminished C=O and C=C, indicating the removal of hemicellulose and lignin. Different chemical treatments resulted in distinguished physical and chemical characteristics. TEM analysis proved that all sample hydrolysed with different H_2SO_4 concentration has a nano size. The image of 12NC best depicts the optimum effect of H_2SO_4 towards the success of NC extraction. From crystallinity analysis, the higher the concentration of H_2SO_4, the higher the CI of NC samples. Lastly, 16NC had the lowest thermal degradation at 325 °C among other NC samples.

ACKNOWLEDGEMENT

The authors are grateful to the Ministry of Higher Education for the financial support provided for this research with grant number FRGS/1/2022/STG04/ UITM/02/10.

REFERENCES

1. Hossain, M. I. M., Zaman, H. and Rahman, T. (2018) Derivation of nanocellulose from native rice husk. *Chemical Engineering Research Bulletin*, **20(1)**, 19–22.

2. Sawawi, M., Sudirman, U., Sahari, S. K., Yusof, M., Andrew, M., Razali, N. T., Sapawi, R. and Kipli, K. (2018) The effect of silane treatmenton rice husk / Phenol formaldehyde particleboard mechanical properties. *International Journal of Engineering & Technology*, **7(3)**, 53–57.

3. Noremylia, M. B., Mohamad, Z. H. and Ismail, Z. (2022) Recent advancement in isolation, processing, characterization and applications of emerging nanocellulose: A review. *International Journal of Biological Macromolecules*, **206**, 954–976.

4. Yu, M., Yang, R., Huang, L., Cao, X., Yang, F. and Liu, D. (2012) Preparation and characterization of bamboo nanocrystalline cellulose. *BioResources*, **7(2),** 1802–1812.

5. Iorfa, T. F., Iorfa, K. F., McAsule, A. A. & AKaayar, M. A. (2020) Extraction and characterization of nanocellulose from rice husk. *SSRG International Journal of Applied Physic.*, **7(1**), 117–122.

6. Phanthong, P., Reubroycharoen, P., Hao, X., Xu, G., Abudula, A. and Guan, G. (2018) Nanocellulose: Extraction and application. *Carbon Resources Conversion*, **1(1)**, 32–43.

7. Kaur, M., Kumari, S. and Sharma, P. (2018) Chemically modified nanocellulose from rice husk: Synthesis and characterization. *Advances in Research*, **13(3)**, 1–11.

8. Benini, K. C. C. D. C., Voorwald, H. J. C., Cioffi, M. O. H., Rezende, M. C. R. and Arantes, V. (2018) Preparation of nanocellulose from Imperata brasiliensis grass using taguchi method. *Carbohydrate Polymers*, **192**, 337–346.

9. Bacha, E. G. and Demsash, H. D. (2021) Extraction and characterization of nanocellulose from Eragrostis Teff Straw. *Research square*, 1-19.

10. Rashid, S. and Dutta, H. (2020) Characterization of nanocellulose extracted from short, medium, and long grain rice husks. *Industrial Crops and Products*, **154**, 2–10.

11. Bolat, F., Ghitman, J., Necolau, M. I., Vasile, E. and Iovu, H. (2023) A comparative study of the impact of bleaching method on production and characterization of cotton origin nanocryatalline cellulose by acid and enzymatic hydrolysis. *Polymers*, **15 (3446)**, 1–18.

12. Chen, L., Wang, Q., Hirth, K., Baez, C., Agarwal., U. P. and Zhu, J. Y. (2015) Tailoring the yield and characteristic of wood cellulose nanocrystals (CNC) using concentrated sulfuric acid. *Cellulose*, **22**, 1753–1762.

13. Islam, S. M., Kao, N., Bhattacharya, S. N., Gupta, R., Choi, J. Y. (2018) Potential aspect of rice husk biomass in Australia for nanocrystalline cellulose production. *Chinese Journal of Chemical Engineering*, **26**, 465–476.

14. Royan, N. R. R., Sulong, A. B., Yuhana, N. Y., Chen, R. S., Ab Ghani, M. H. and Ahmad, S. (2018) UV/O_3 treatment as a surface modification of rice husk towards preparation of novel bio-composites. *PLoS One*, **13(5)**, **e0197345**, 1–17.

15. Rashid, E. S. A., Gul, A., Yehya, W. A. H. and Julkapli, N. M. (2021) Physico-chemical characteristics of nanocellulose at the variation of catalytic hydrolysis process. *Heliyon*, **7**, 1–7.

16. Hafemann, E., Battisti, R., Bresolin, D., Marangoni, C. and Machado, R. A. F. (2020) Enhancing chlorine-free purification routes of rice husk biomass waste to obtain cellulose nanocrystals. *Waste Biomass Valorization*, **11**, 6595–6611.

17. Shaheen, T. I. and Emam, H. E. (2018) Sono-chemical synthesis of cellulose nanocrystals from wood sawdust using acid hydrolysis. *International Journal of Biological Macro-molecules*, **107**, 1599–1606.

18. Trache, D., Tarchoun, A. F., Derradji, D., Hamidon, T. S., Masruchin, N., Brosse, N. and Hussin, M. A. (2020) Nanocellulose: From fundamental to Advanced Applications. *Frontiers in Chemistry*, **8**, 1–33.

19. Cao, X. W., Ding, B., Yu, J. Y., Al-Deyab, S. S. (2012) Cellulose nanowhiskers extracted from TEMPO-oxidized jute fibers. *Carbohydrate Polymers*, **90 (2)**, 1075–1080.

20. Barbash, V. A., Yaschenko, O. V., Alushkin, S. V., Kondratyuk, A. S., Posudievsky, O. Y. and Koshechko, V. G. (2016) The effect of mechanochemical treatment of the cellulose on characteristics of nanocellulose films. *Nanoscale Research Letters*, **11(410)**, 1–8.

21. Wu, Y., Luo, C., Wang, T., Yang, Y., Sun, Y., Zhang, Y., Cui, L., Song, Z., Chen, X., Cao, X., Li, S. and Cai, G. (2024) Extraction and characterization of nanocellulose from cattail leaves: Morphological, microstructural and thermal

properties. *International Journal of Biological Macromolecules*, **255(128123)**, 1–9.

22. Islam, M. S., Kao, N., Bhattacharya, S. N., Gupta, R., and Bhattacharjee, P. K. (2017) Effect of low-pressure alkaline delignification process on the production of nanocrystalline cellulose from rice husk. *Journal of the Taiwan Institute of Chemical Engineers*, **80**, 820–834.

23. Hafid, H. S., Omar, F. N., Zhu, J. and Wakisaka, M. (2021) Enhanced crystallinity and thermal properties of cellulose from rice husk using acid hydrolysis treatment. *Carbohydrate Polymers*, **260**, 1–12.

24. Collazo-Bigliardi, S., Ortega-Toro, R. and Boix, A. C. (2018) Isolation and characterisation of microcrystalline cellulose and cellulose nanocrystals from coffee husk and comparative study with rice husk. *Carbohydrate Polymers*, **191**, 205–215.